# Carbon Clusters: Thermochemistry and Electronic Structure at High Temperatures

Maitreyee P. Sharma,*,† Richard L. Jaffe,‡ and Marco Panesi*,†

†*Department of Aerospace Engineering, University of Illinois, Urbana-Champaign*

‡*NASA Ames Research Center*

E-mail: sharmap2@illinois.edu; mpanesi@illinois.edu

**Abstract**

This paper studies the thermochemistry and electronic structure of small carbon clusters and hydrocarbons which are major constituents of pyrolysis gases released into the boundary layer of ablating heat shields. Our focus lies on clusters of up to four carbon atoms. Among other molecules, thermochemsitry data for molecules like $C_3H$ and $C_4H$ has been determined using the W1 method. These molecules have very limited data recorded in literature thereby necessitating new and accurate computations of required properties. A study of electronically excited states of these molecules computed using the EOM-CCSD method revealed $C_4$ and $C_4H$ to be potential sources of radiation absorption in the boundary layer. The excited electronic states of interest are studied further to obtain their optimum geometries, rotational constants and vibrational frequencies. Moreover, we also study the effect of low-lying excited electronic states on the partition function to assess their effect on thermodynamics of these pyrolysis gases in the high temperature regime. Neglecting the excited electronic states records a maximum difference of 12% in the computed $C_p$ values. Finally, comparisons of the equilibrium mole fractions obtained using the thermodynamics computed in this paper with the existing state-of-the-art tables used for hypersonic applications (for example JANAF and Gurvich Tables) show an order of magnitude difference in the mixture compositions. It is shown

that the rhombic isomer of $C_4(^1A_g)$ which is energetically close to the ground state ($^3\Sigma_g^-$) and usually neglected in composition calculations, contributes to 28% increase in the equilibrium mole fraction of $C_4$ molecule.

# 1 Introduction

The occurrence of carbon clusters in various scientific fields has led to considerable interest in the prediction of the properties of these molecules both experimentally and theoretically. The earliest efforts to compute the electronic structures of linear carbon clusters were undertaken by Pitzer and Clementi.[1,2] The paper of Raghavachari and Binkley[3] was amongst the earliest works in the dawn of computational chemistry that discussed the structure and frequencies of small carbon clusters (upto 10 carbon atoms) based on HF and CCS(DT) methods. These calculations were improved by Martin et al.[4–6] who used the CCSD(T) method with correlation-consistent basis sets. On the side of experiments, Gingerich et al.[7] determined the formation enthalpies of small linear carbon clusters using high-temperature Knudsen effusion mass spectroscopy. The measured mole fractions of various carbon clusters in the carbon vapor at temperatures between 2500K and 3000K were used to determine the equilibrium constants, and, ultimately, to back out the formation enthalpies. A 1998 review paper by Van Orden and Saykally[8] surveyed the properties of ground and excited electronic states of carbon clusters, along with the computational methods and experiments that were designed to obtain these values. Since that year, numerous computational studies of the ground states of $C_n$ species have been published. The most notable for $C_n$ species is by Karton et at.[9] Using state of the art quantum chemistry methods described in the next section, the estimated uncertainties in the formation enthalpies at 0K for $C_n$ (n = 2,10) were estimated to be less than $\pm$ 0.5 kcal/mol. The importance of small carbon clusters can be seen when looking at their occurrence in the interstellar medium. Owing to this, a recent review of the band systems of $C_2$ has been published by Schmidt.[10]

Study of excited electronic states of larger carbon clusters like $C_4$ and $C_4H$ has been rather

limited. An early study by Pacchioni et al.[11] performed single reference and multi-reference calculations to study the ground and excited states of $C_4$ and $C_5$. Vertical excitation energies were calculated up to 2.8 eV, identifying the lowest electronic transitions in the ground linear and rhombic states of $C_4$. Mülhäusser et al.[12] performed multi-reference configuration interaction (MRCI) calculations to obtained vertical excitation energies up to 6.5 eV for $C_4$. Two transitions in the linear geometry were observed in this energy range. These calculations are used to benchmark calculations done in the present work. For $C_4H$, Graf et al.[13] studied the ground and excited electronic states up to 8 eV. The excited state energies were estimated using multi-reference second order perturbation theory. The harmonic frequencies for vibration were estimated for the ground and first four excited electronic states. However, they were unable to obtain the optimized geometries for the second, third and fourth excited electronic states. Fortenberry et al.[14] also obtained the excitation energies up to 8 eV for $C_2H$ and $C_4H$. The purpose of this work was to benchmark the coupled cluster calculations. Fortenberry and co-authors concluded that the coupled cluster methods are not adequate to obtain high lying electronic states for these molecules and also pointed the issue of spin contamination in these calculations.

In hypersonics particularly, the interest in carbon species arises from the use of ablating carbonaceous heat shields. Returning spacecrafts can attain entry speeds of 10-13 km/s which results in intense radiation in the shock layer that is directed towards the spacecraft fore body. The radiation is predominantly due to atomic N(I) and O(I) lines[15] with the main spectral feature being the intense 174.29 nm line of atomic nitrogen. Ablating heat shields undergo pyrolysis and sublimation resulting in the formation of a gas layer which carries away some of the incident radiation via convention thereby mitigating the radiative heat flux on the spacecraft. Another source of radiation attenuation is by absorption of a portion of the incoming radiative heat flux from the shocked gases by the pyrolysis gases in the boundary layer. Accounting for this absorption can cause a reduction in the predicted radiative heat flux impinging on the spacecraft, leading to more efficient designs for heat shields and predictive modeling of hypersonic re-entry flights.

Some early shock tube experiments done by Prakash and Park estimated that the reduction in

radiative flux could be as large as 12.5%[16] with strong absorption of VUV radiation at temperatures between 3500-4000K. These experiments were conducted with shock heated acetylene and methane and the absorption was attributed to $C_3$[16] and $C_2H$.[17] Studying the composition of the pyrolysis gases injected into the boundary layer by carbonaceous ablating heat shields revealed that $C_3$ is the predominant pyrolysis species.[18,19] Having a prominent spectral feature in the VUV (centered at 160 nm[20]), it is proposed that $C_3$ can absorb the radiative heating due to emission by atomic nitrogen at 174.29 nm.[18]

The relevance and importance of studying small carbon clusters and hydrocarbons, $C_n$ and $C_nH$ (n = 1,5), has urged to authors to study their properties in this paper. Our focus primarily lies on the thermodynamics and spectroscopic properties of these molecules at high temperatures relevant to ablating boundary layer conditions since these are major constituents of the pyrolysis gases. Smaller molecules like $C_2$, $C_3$ and $C_2H$ have been studied extensively and hence these molecules are used to validate the applicability of the quantum chemistry methods used in this paper for carbon clusters. Their properties are fairly well known for temperatures up to 10,000K with $C_3$ being proven to be the most abundant carbon cluster from temperatures between 2,000K to 4,000K. For these smaller carbon clusters, we go a step further and study the effects of low lying excited electronic states on the partition function and in turn the thermodynamics at high temperatures. For $C_4$, $C_4H$ and other larger carbon clusters and hydrocarbons, we compute the thermodynamics using the W1 method[21] from Gaussian 16[22] software package. All the excited electronic states are computed using the EOM-CCSD method.[23–25]

The paper is organised in two major sections. The first section involves the calculation of thermochemistry data for the ground state of carbon clusters and hydrocarbons including the study of the effect of excited electronic states. This data is then used to compare the equilibrium compositions of pure carbon and acetylene mixtures with state of the art thermodynamic tables used in hypersonics today. The second part is focused on studying the excited electronic structure of the $C_3$, $C_4$ and $C_4H$ molecules. These molecules have been chosen on basis of their absorption features in the VUV region that closely match the emission features of atomic oxygen and nitrogen. An

overview of the theory and computational methods of quantum mechanics used for the calculation of properties of various molecules is presented in Section 2. Subsection 2.2 discusses the quantum chemistry methods used to compute the excited electronic state energies and transition moments whereas subsection 2.1 discusses the tools from statistical mechanics used to compute the thermodynamic properties. The results are presented in section 3 followed by the concluding remarks in section 4.

# 2 Theoretical and Computation Methods

The past few years have marked phenomenal progress in the development of accurate quantum chemistry methods, so much so that their accuracy is comparable or better than the corresponding experiments. Consequently, an important outcome has been in the advancement of ab-intio calculations of thermochemistry data. In the current study, we utilize these quantum chemistry methods in three different ways as part of a larger effort to characterize the gaseous environment surrounding the spacecraft during atmospheric entry. To start off, we compute the formation enthalpies of the carbon clusters and hydrocarbons present in the boundary layer of an ablating heat shied. Second, we use these methods to obtain free energy and entropy to compute the equilibrium composition of these gases at relevant conditions and finally, the electronic absorption spectrum of these molecules are computed to identify candidates that can play a role in mitigating the radiative heat flux that impinges on the vehicle. This includes computing the excitation energies between the ground and excited electronic states and the electronic transition dipole moments between these states in order to identify strong absorption and emission transitions.

These methods provide approximate, but accurate, solutions of the Schrödinger equation whose analytical solution cannot be found for multi-electron molecules. Since the coupled dynamics of the nuclei and electrons is a complex problem, the Born-Oppenheimer approximation is invoked to decouple the electrons and nuclei. The electronic structure is then calculated keeping the nuclei stationary. The standard procedure employed in these methods is approximation of the Hamil-

tonian to account for all the important contributions to the electronic energy. The following two subsections describe the methods in detail.

## 2.1 Ground State Calculations

Since the primary interest of this paper lies in the chemistry of the boundary layer species, it is natural to first look at the mole fractions of individual species in the boundary layer which provides an estimate of the chemical composition. In order to compute the equilibrium composition, we are required to know the enthalpy and entropy of each species over the relevant range of temperature and pressure. These quantities of interested are obtained from the molecular partition function. The ground state equilibrium geometry and harmonic vibrational frequencies enable approximate calculation of the harmonic oscillator-rigid rotor partition functions. Additional calculations can provide the anharmonic vibration energy levels and rotation-vibration coupling constants, which permit more accurate ro-vibrational partition functions to be determined.

In an earlier paper by the authors,[26] the focus lay on using the Gn methods proposed by Curtiss et al.[27–29] These methods fall under the umbrella of hybrid methods. Hybrid methods determine the energies of molecules at their equilibrium geometries by combining results obtained from high-level correlation methods (like quadratic configuration interaction theory (QCISD) and coupled cluster theory (CCSD)) using small atomic orbital basis sets with results from lower level methods (like MP2 and MP4) using a large basis set. To increase the accuracy of the final result, an empirical additive correction term is determined as follows. For a large test set of small molecules, a specific property(e.g., atomization energy) is computed using a particular hybrid method and compared with reference values based on experiment. The empirical term is the correction factor that brings the test set results into the best overall agreement with the experimental data.

To determine the enthalpy of formation, a series of accurate calculations are carried out using the W1 method.[21] This method is another composite quantum chemistry method used to compute the thermodynamics in this paper. This method includes valence electron correlation at the level of CCSD and CCSD(T) calculations, inner core electron correlation at the levels of CCSD(T)

using the Dunning basis set, scalar relativistic correction as well as spin-orbit coupling. Overall more correlation energy is captured in this method when compared to the CCSD method using an aug-cc-pVTZ (augmented correlation-consistent valence triple-$\zeta$) atomic orbital basis set. It has a mean absolute error of approximately 0.3 kcal/mol and unlike other methods includes only a single, molecule-independent empirical parameter. It has been developed for molecules composed of atoms from the first two rows of the periodic table which encompasses the molecules being studies in this work.

The methods mentioned above give the total electronic energy ($\varepsilon_0$), which along with zero-point vibration energy is used to calculate the atomization energy, $D_0$(M) at T = 0K, using,

$$D_0(M) = \sum x\ \varepsilon_0(X) + \sum y\ \varepsilon_0(Y) - \varepsilon_0(M) \tag{1}$$

where x and y stand for number of X and Y atoms in molecule M. The enthalpy of formation ($\Delta_f$ H $^o$) and Gibbs free energy ($\Delta_f$ G $^o$) of the molecules at 0K are computed by,

$$\Delta_f H^o(M,0K) = x\ \Delta_f H^o(X,0K) + y\ \Delta_f H^o(Y,0K) - D_0(M), \tag{2}$$

$$\Delta_f G^o(M,0K) = \Delta_f H^o(M,0K) - T[S^o(M,0K) - \sum_{\text{atoms}} S^o(X,0K)]. \tag{3}$$

Since all thermodynamic properties can be derived from the molecular partition function,[30] the harmonic frequencies and rotational constants computed are used to determine the internal molecular partition function. It is common practice to factor $Q_{\text{int}}$ into vibration, rotation and electronic components,

$$Q_{\text{int}} = Q_{\text{rot}} \times Q_{\text{vib}} \times Q_{\text{elec}}, \tag{4}$$

and use the harmonic oscillator-rigid rotor approximation (HO-RR) for $Q_{\text{rot}}$ and $Q_{\text{vib}}$. If the energy difference between the ground and first electronic states is much larger than $k_B$T, where T

is the temperature, this assumption is reasonable. For the electronic partition function, the energies of the excited electronic states are calculated as discussed in the following Sec. 2.2. The total partition function, $Q_{TOT}$, is the product of the translation mode partition function, $Q_{tr}$, and the internal mode partition function, $Q_{int}$.

In this paper, we assume ideal gas behavior in the boundary layer and evaluate the thermodynamic functions at the standard state. The standard state specific heat is given by,[30]

$$C_P^o = C_P^{oINT} + \frac{5}{2}R, \tag{5}$$

$$C_P^{oINT} = RT^2 \frac{\partial^2 \ln Q_{int}(T)}{\partial^2 T} + 2RT \frac{\partial \ln Q_{int}(T)}{\partial T}. \tag{6}$$

The superscript '$o$' indicates standard state and $\frac{5}{2}$R is the translation contribution to $C_P^o$.

For standard state enthalpy we get[30]

$$H^o(T) = H^o(0) + RT^2 \frac{\partial \ln Q(T)}{\partial T}, \tag{7}$$

where $H^o(0)$ must include the formation enthalpy ($\Delta_f H^o$).

Finally, the standard state entropy is given by,[30]

$$S^o(T) = R \frac{\ln Q(T)}{N} + RT \frac{\partial \ln Q(T)}{\partial T}. \tag{8}$$

It is convenient to use T = 0K as the reference temperature because only the lowest energy level of each species contributes to the thermodynamic functions.

The equilibrium constant is then expressed in terms of the partition function as,[30]

$$K_{\text{eq}} = \frac{Q_C^c \, Q_D^d}{Q_A^a \, Q_B^b} \tag{9}$$

for the following example reaction,

$$a\,A + b\,B \rightarrow c\,C + d\,D. \tag{10}$$

The species of interest in this paper are small carbon clusters and hydrocarbons. For even numbered carbon clusters, both the triplet ground states as well as the low lying singlet excited state are studied. For larger carbon clusters and hydrocarbons, all nearly iso-energetic isomers are included as well.

The softwares PLATO[31,32] and ROSSDAG developed at University of Illinois, Urbana-Champaign, are used to compute the thermodynamic properties and equilibrium compositions. The equilibrium calculations are carried out for a range of boundary layer temperatures.

## 2.2 Electronic Structure Calculations

One of the focuses of this paper is to characterize the excited electronic states of carbon clusters and hydrocarbons. This is done in order to determine their contribution to the enthalpy and entropy of the chemical system and to identify excited states with strong optical absorption transitions from the ground state that could take place in the boundary layers of re-entry vehicles.

For the calculation of excited electronic states, we use the equations of motion coupled cluster singles doubles (EOM-CCSD) method.[23–25] This method is based on linear response theory. Here, the effective Hamiltonian operator is obtained by a similarity transformation of the ground state Hamiltonian operator. This nonlinear transformation tends to include the effects of higher excitations thereby recovering more of the correlation energy in the excited states and, as a result, gives more accurate excitation energies. These calculations generally have an error of less than 0.1-0.3 eV in the excitation energies ($\sim$ 2.39 - 7 kcal/mol) for the low-lying electronic states and the relative state ordering is usually better when compared to time-dependent density functional theory (TD-DFT).

The calculations are done in the following way. As an initial guess for the EOM-CCSD optimization calculations, we use the result from time-dependent density functional theory(TD-DFT) obtained using the B3LYP hybrid functional[33] and the augmented correlation-consistent valence triple-$\zeta$ (aug-cc-pVTZ) atomic orbital basis set.[34,35] The EOM-CCSD calculation is carried out using the same aug-cc-pVTZ atomic orbital basis set. The ground state energy, frequency and

geometry is obtained using the CCSD method with aug-cc-pVTZ basis set to be consistent with the EOM-CCSD calculations. The oscillator strength, which determines the strength of the optical transition, is computed between the ground electronic state and all of the excited states to identify strong electronic transitions. For the molecules of interest, the first 35 excited electronic states are computed using Gaussian16 package.[22] This provides an effective cut off energy of approximately 11 eV, which corresponds to a minimum absorption wavelength of 112 nm, thereby covering the VUV range of wavelengths for radiation.

For the species with strong electronic transitions in the VUV region, the bending and stretching potentials of the excited electronic states are mapped out at different molecular configurations using EOM-CCSD method. For the promising radiation blocking molecules, the excited states of interest are optimized at the EOM-CCSD level of theory and the harmonic frequencies of these states are computed. This data will be useful in future studies to quantify the radiation being absorbed by these molecules in the boundary layer.

The main molecules focused in this study are $C_4$ and $C_4H$ due to the promising spectral features and the lack of available data. For $C_4$, the optimization of the excited state is done using numerically computed Jacobian. In the case of $C_4H$, the excited state minimum is found to have a bent geometry. The geometry optimization for this excited electronic state is carried out in two parts. First, the middle carbon-carbon bond (CC-CCH) is fixed at different values and a relaxed PES optimization calculation is carried out. Mapping out the potential energy curve for the relaxed PES at different bond lengths indicates the nature of the surface and approximate position of the minimum. The full molecule geometry is then optimized with the initial guess being the approximate minimum observed earlier. All the calculations are carried using the augmented correlation-consistent valence triple-$\zeta$ (aug-cc-pVTZ) atomic orbital basis set.[34,35]

# 3 Results and discussion

The results section is divided into four main subcategories. The first section is focused on the ground state thermodynamic properties. Before computing the thermochemical properties and spectral features of the test molecules, $C_4$ and $C_4H$, a validation study is done to compare the results with those available in the literature. The molecules used in the validation study are mainly smaller carbon clusters and hydrocarbons. We next discuss the effects of low lying electronic states on the thermochemistry since the low lying states become important in the high temperature regime corresponding to the boundary layer during hypersonic reentry.

Further in this section, molecules with favourable spectral characteristics are recognized using the basic TD-DFT method. The electronic states with high transition probabilities are then studied and optimized using the EOM-CCSD method as mentioned in Section 2.2. Upon the determination of the spectral properties and thermochemitry, equilibrium mole fractions of these species at conditions of the boundary layer are estimated using the thermochemical library, PLATO.[31,32] This estimation is necessary to understand the potential impact these carbon clusters can have on the radiation due to electronic state transitions in atomic species found in the shock layer during hypersonic reentry.

## 3.1 Ground State Thermodynamic Properties

Here, the formation enthalpies obtained from the W1[21] method from Gaussian16[22] are compared with state-of-the-art tables for validation and to shed light on the limitations of these tables. From the W1[21] method, we obtain the total electronic energy along with thermal enthalpy at 0K, denoted by $\varepsilon_0(M)$ in Eqn. 1, which is used to compute the atomization energy of the molecule. Following this calculation, the formation enthalpy of the molecule is computed using Eqn. 2 where the atomic formation enthalpies are taken from Ref. 36. Besides determining $\Delta_f H$ (0 K) from atomization energies, other reactions can be used as well, for example, $C_4 \leftarrow C_2 + C_2$. Computing this quantity using various reactions provides a consistency check. Therefore, validation for the data computed

in this paper is done using Active Thermochemical Tables (ATcT).[37–39] ATcT is a database of thermochemical properties for molecules developed at the Argonne National Laboratory. The properties are calculated by taking a weighted average of values from literature, which include experimental and computational results for various reaction mechanisms. The thermochemical data is also compared to JANAF Tables[40] and Gurvich Thermodynamic Tables[41] whose values are widely used for the prediction of mixture composition in the boundary layer of an ablating heat shield.

The test molecules formation enthalpies have good agreement with ATcT, with differences mostly in a range of $\pm$ 1 kcal mol$^{-1}$ as found in previous studies.[9] Since ATcT enthalpies are based on many different reactions and weighted to give an overall best agreement with different values, their values vary slightly from the values we obtained using the method outlined above. Thermochemical properties for molecules like $C_3H$ and $C_4H$ which are not available in the previously mentioned tables have also been determined in this paper.

Table 1: Comparison of $\Delta_f H$ at 0K with Existing Thermochemical Tables (in kcal mol$^{-1}$)

| Molecule | CBS-QB3 | G4 | W1 | ATcT | JANAF[40] | Gurvich[41] |
|---|---|---|---|---|---|---|
| $C_2(^1\Sigma_g^+)$ | 195.25 | 192.50 | 196.09 | 196.04 $\pm$ 0.06 | 198.19 | 196.56 |
| $C_2(^3\Pi_u)$ | - | - | 198.66 | 197.77 $\pm$ 0.06 | - | - |
| $C_3(^1\Sigma_g^+)$ | 195.68 | 192.91 | 194.73 | 194.68 $\pm$ 0.13 | 193.94 | 198.61 |
| $C_3(^3A1)$ | - | - | 213.80 | 214.84 $\pm$ 0.38 | - | - |
| $C_4(^3\Sigma_g^-)$ | - | - | 252.40 | 251.54$\pm$ 0.16 | - | - |
| $C_4(^1A_g)$ | 252.36 | 248.10 | 251.57 | 250.34 | 230.43 | 244.98 |
| $C_5(^1A_g)$ | 255.4 | 251.45 | 253.23 | - | - | 248.56 |
| $C_2H(^2\Sigma^+)$ | 135.86 | 133.84 | 134.79 | 134.77 $\pm$ 0.04 | 113.27 | 135.04 |

| | | | | | | |
|---|---|---|---|---|---|---|
| CH ($^2\Pi$) | 141.58 | 140.50 | 141.61 | $141.68 \pm 0.03$ | 141.17 | 141.98 |
| $C_3H(^2\Pi)$ | 171.39 | 169.01 | 170.03 | $171.59 \pm 0.19$ | - | - |
| $C_3H(^2B_2)$ | 175.66 | 170.66 | 171.94 | $169.86 \pm 0.26$ | - | - |
| $C_4H$ ($^2\Sigma_g^+$) | 191.68 | 190.54 | 190.49 | - | - | - |
| $C_4H$ (Cyclic) | 215.29 | 212.02 | 212.24 | - | - | - |

## 3.2 Effect of low lying electronic states on thermochemistry at high temperatures

For the purpose of studying the effect of low-lying electronic states on thermochemistry, for the molecules $C_2$, $C_3$ and $C_4$, the harmonic frequencies and rotational constants have been computed for the low lying electronic states. The data for the $C_2$ molecule has been obtained from the book by Huber and Herzberg.[42] The effects on thermochemistry are studied by considering the following cases; (i) solely the ground state, (ii) ground state and low lying electronic states with the same harmonic and rotational frequencies for all the levels, done when factorizing the partition function into translation, vibration, rotation and electronic modes, and (iii) ground state and low lying electronic states with the harmonic and rotational frequencies computed for each state separately.

Table 2 gives the equilibrium geometry, rotational constants and vibrational frequencies of the ground and first five excited electronic states of $C_3$. The ground state and first four electronic states have linear geometries with four normal modes of vibrations. The first $^1\Pi_g$ state has an optimum geometry that slightly deviates from the linear geometry. In this state, as a result of the Renner-Teller effect, the degenerate $\pi$ vibration modes are split into two non-degenerate components. The last state, $^1\Sigma_u^+$, has a bent geometry and corresponds to the strong transition in the VUV region of the $C_3$ absorption spectrum. The energies of these states obtained with the MRCI method and

EOM-CCSD method are given and discussed in the following section. Similarly, Table 3 gives the properties of the ground and first few electronic states of the $C_4$ molecule. The first $^3Pi_u$ state has a slightly bent geometry.

Table 2: $C_3$ optimum bond lengths [A], energy at optimum geometry [eV], rotational constants [GHz] and normal mode frequencies [$cm^{-1}$] for the ground state and the first 4 excited electronic states. The calculations are done using the W1[21] and EOM-CCSD[23–25] method for the ground state and excited electronic states, respectively.

| Bond Lengths | | $^1\Sigma_g^+$ | $^1\Pi_u$ | $^1\Sigma_u^-$ | $^1\Delta_u$ | $^1\Pi_g$ |
|---|---|---|---|---|---|---|
| C-C | | 1.2876 | 1.2919 | 1.3588 | 1.3607 | 1.2744 |
| ∠C-C-C | | 180 | 180 | 180 | 180 | 179.97 |
| Electronic Energy | | 0.0 | 3.2909 | 3.6286 | 3.6601 | 4.5090 |
| Rotational Constant | | 12.6996 | 12.7130 | 11.4050 | 11.3732 | 12.9657 |
| Vibration Type | Symmetry | | | | | |
| Asymm. stretch | $\sigma_u$ | 2144.7779 | 802.0028 | 1476.4532 | 1468.1122 | 2486.0658 |
| Symm. stretch | $\sigma_g$ | 1239.7376 | 1237.2944 | 1052.6415 | 1049.8553 | 1305.0620 |
| Bending | $\pi_u$ | 102.1667 | 199.4862 | 322.3461 | 318.6066 | 612.6446 |
| Bending | $\pi_u$ | 102.1667 | 198.4967 | 322.1659 | 316.2072 | 526.9258 |

Table 3: $C_4$ optimum bond lengths [A], energy at optimum geometry [eV], rotational constants [GHz] and normal mode frequencies [$cm^{-1}$] for the ground state and the first 4 excited electronic states. The calculations are done using the W1[21] and EOM-CCSD[23–25] level of calculation for the ground state and excited electronic states, respectively.

| Bond Lengths | | $^3\Sigma_g^-$ | $^3\Pi_g$ | $^3\Pi_u$ | $^3\Delta_u$ | $^3\Sigma_u^+$ |
|---|---|---|---|---|---|---|
| C1-C2 | | 1.305 | 1.2518 | 1.2589 | 1.2911 | 1.2909 |
| C2-C3 | | 1.2863 | 1.3249 | 1.3148 | 1.4209 | 1.4230 |
| C3-C4 | | 1.305 | 1.2518 | 1.2589 | 1.2911 | 1.2909 |
| ∠C1-C2-C3 | | 180 | 180.0 | 179.98 | 180 | 180 |
| ∠C2-C3-C4 | | 180 | 180.0 | 179.98 | 180 | 180 |
| Electronic Energy | | 0.0 | 1.2761 | 1.5443 | 2.4731 | 3.42688 |
| Rotational Constant | | 4.9997 | 5.034488 | 5.1305 | 4.5930 | 4.6630 |
| Vibration Type | Symmetry | | | | | |
| Symm. Stretch | $\sigma_g$ | 2124.2059 | 2075.5110 | 2119.6917 | 2026.3267 | 2036.4871 |
| Asymm. Stretch | $\sigma_u$ | 1594.6451 | 1540.8747 | 2617.9614 | 1813.9988 | 1817.1298 |
| Symm. stretch | $\sigma_g$ | 940.1935 | 891.8366 | 972.2412 | 816.0707 | 818.3672 |
| Bending, Zig-Zag | $\pi_g$ | 375.3630 | 629.6849 | 615.4088 | 632.3407 | 529.7626 |
| Bending, Zig-Zag | $\pi_g$ | 375.3630 | 629.6847 | 109.8485 | 632.3296 | 529.7626 |
| Scissoring, Outer C-C | $\pi_u$ | 176.5907 | 141.2258 | 371.7951 | 173.6796 | 140.7875 |
| Scissoring, Outer C-C | $\pi_u$ | 176.5907 | 141.2233 | 314.8613 | 173.6178 | 140.7875 |

Figure 1 demonstrates the comparison of non-dimensional $C_p$ as well as $\Delta H$ for the different cases discussed above. When considering only the ground state(dashed lines), as expected, the $C_p$ is lower since the effects of the higher electronic states are completely neglected when computing the partition function. The dotted lines correspond to case (ii) and the solid lines correspond to case (iii). Having level specific rotation and vibration frequencies lead to some differences in the specific heat however, these differences are not very large in the temperature range of our interest. The important outcome of this comparison is that although having a level specific HO-RR model does not have a large effect on thermochemistry, it is still important to consider the low lying electronic states of the molecule since they get populated at these high temperatures thus affecting the thermochemistry. In the case of $C_2$, the difference is large and up to 12% when going from the ground state to including low-lying excited states, although for case (ii) and (iii) the differences are insignificant (up to 2%). A similar comparison for $C_3$ and $C_4$, shown in Fig. 1b and 1c, leads to the

observation that the differences between case (ii) and case (iii) are also important particularly at higher temperatures as the excited states get more populated. These differences are up to 23%. In the case of $C_4$, due to the large size of the molecule, slightly non-linear optimum geometries of the excited states and the low-lying first excited electronic state, these differences are accentuated even at lower temperatures. Figure 1d shows a comparison of the enthalpies for the three molecules. As can be observed, the effects on the enthalpy are rather negligible.

Finally to demonstrate the effect of these differences on quantities of interest, Fig. 1e, shows a comparison of the equilibrium mole fractions of a pure carbon vapor considering the 3 cases. The plots are shown in both log and linear scale. As the temperature increases, the differences between the compositions become more visible. For $C_4$, the differences in the thermodynamic properties are more important at higher temperatures, however, the mole fractions of $C_4$ in a pure carbon vapor decline quickly above 5000K. Therefore, the differences in the mole fractions are not very significant.

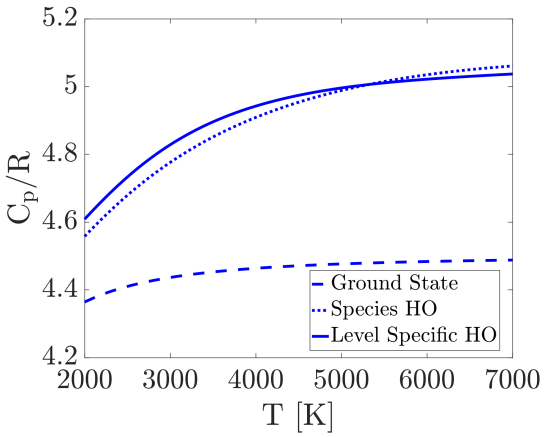


(a) $C_2$

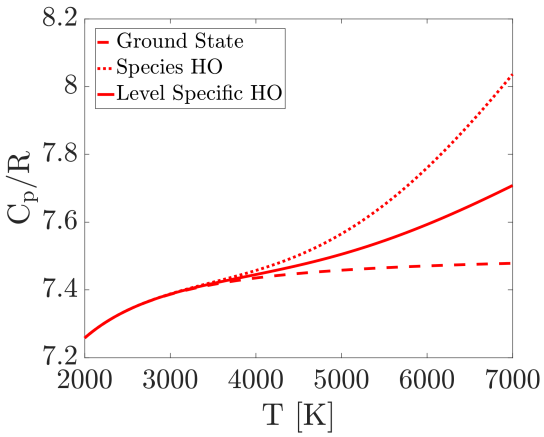


(b) $C_3$

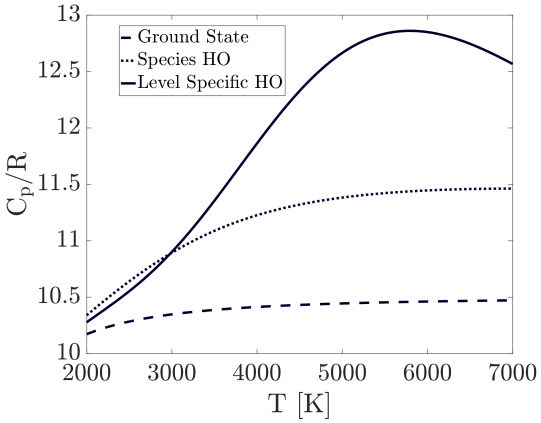


(c) $C_4$

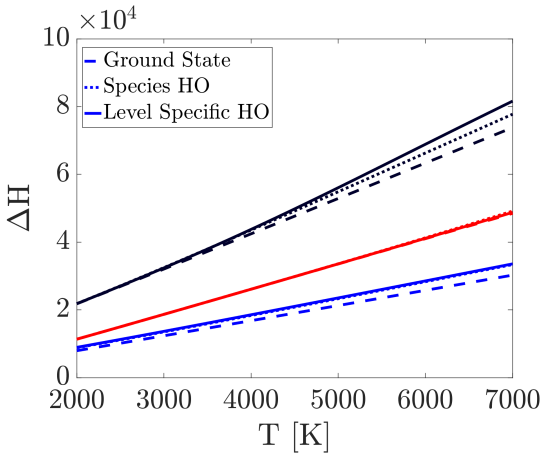


(d) $\Delta H$

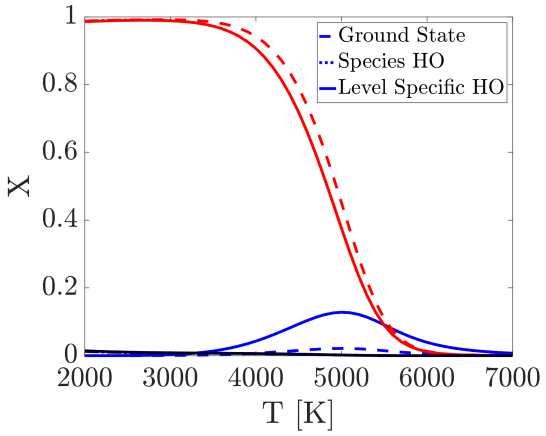


(e) Equilibrium Composition - Linear Scale

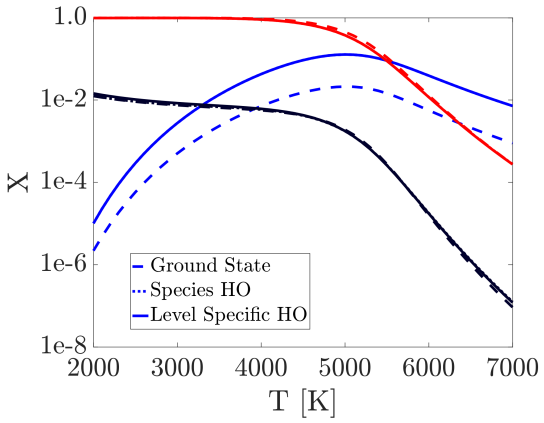


(f) Equilibrium Composition - Log Scale

Figure 1: Effect of low lying electronic states on specific heat ($C_p$) and enthalpy ($\Delta H$). In the figures above, the properties of $C_2$, $C_3$ and $C_4$ are represented in blue, red and black lines respectively. Ground state properties are represented by dashed lines(- -), case (ii) by dotted lines(:) and case (iii) by solid lines(-).

## 3.3 Excited Electronic States Potential Energy Curves

### 3.3.1 $C_3$

$C_3$ has been studied previously by Jaffe et. al.[18] They identified a strong transition from the ground state to the first $^1\Sigma_u^+$ electronic state that can be effective in absorption of the radiation flux for the wavelength range 160-190 nm. Following their work, the electronic energy states of $C_3$ have been computed via the MRCI method using the MolPro software package.[43] The results are compared to the calculations of the TD method. For these calculations, the aug-cc-pVTZ basis set is used and the MRCI energies are computed for $D_{\infty h}$ symmetry. The ground state of the molecule has the $D_{\infty h}$ symmetry and an optimum bond length of 1.2876 Angstrom. Figure 2b represents the bending potential for $C_3$ molecule obtained using TD method with augmented correlation-consistent valence triple-$\zeta$ (aug-cc-pVTZ) basis set. The diamond markers in the figure show the MRCI results from Ref. 18. This comparison shows that the results are in agreement for some of the states. However, a few states are missing when using the TD method to obtain the excited electronic state. Due to the deficiency of the TD method further calculations are done using the MRCI method. It can be pointed out that the $^1\Sigma_u^+$ state, state number 8 in the figure has a minimum near $\phi = 120^\circ$. Although, the TD method is able to predict the low lying states within chemical accuracy, it is missing states and the errors in the high lying states increases upto 1.5 eV.

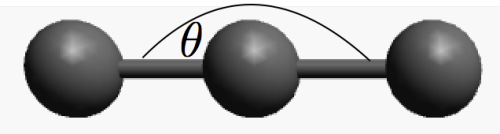


(a) $C_3$ Molecule Ground State

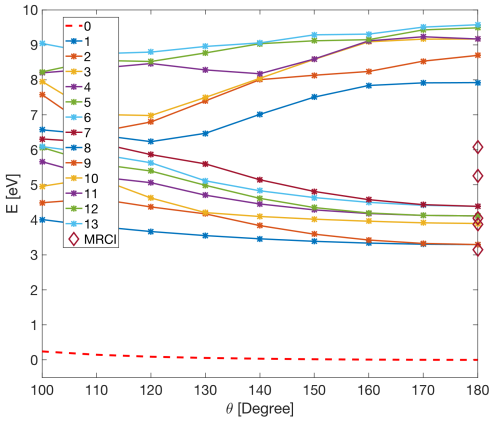


(b) Bending potential from TD calculations

Figure 2: Excited Electronic States potential for $C_3$

A comparison of the $C_3$ electronic energies obtained from the TD-DFT, EOM-CCSD and MRCI methods is given in Table 4.

Table 4: Comparison of energies obtained from the TD-DFT, EOM-CCSD and MRCI methods at the optimum ground state geometry. The energies are measured from the ground state minimum.

| State | MRCI | EOM-CCSD | TD-DFT | $f_{EOM}$ |
|---|---|---|---|---|
| $^1\Sigma_g^+$ | 0.0 | 0.0 | 0.0 | - |
| $^1\Pi_u$ | 3.2376 | 3.3996 | 3.2941 | 0.0233 |
| $^1\Sigma_u^-$ | 4.0071 | 4.0041 | 3.8962 | - |
| $^1\Delta_u$ | 4.0364 | 4.0245 | 4.1123 | - |
| $^1\Pi_g$ | 4.1055 | 4.5112 | 4.3857 | - |
| $^1\Delta_g$ | 5.3793 | M | M | - |
| $^1\Sigma_g^+$ | 6.0671 | M | M | - |
| $^1\Sigma_u^+$ | 6.5242 | 8.0433 | 7.9210 | 1.3033 |

### 3.3.2 $C_4$

As already known, the ground state of $C_4$ is a linear triplet state with a low lying energetically close singlet state which has a rhombus geometry. Since the spectral features of interest to this work are observed in the linear triplet state, hereafter our focus is primarily the triplet states of $C_4$. The optimum geometry of the triplet ground state of $C_4$ is given in Table 3. The optimized bond length values for the ground state have been calculated earlier in [44] using the coupled cluster method and are in good agreement with our calculations. These values also match the experimental values given in the review by Orden and Saykally.[8] The optimum geometry for the excited state of interest(SoI) is given in Table 5 along with the rotational constant and normal mode vibration frequencies. The excited state has a linear geometry with bond lengths slightly higher than the ground state. This is expected due to the larger spread of the electron cloud around the atoms. The molecule in the excited state belongs to the $D_{\infty h}$ point group.

In an effort to be able to identify the linear and rhombic states of $C_4$, Mühlhäuser et al.[12] computed the vertical electronic spectrum of $C_4$ using MRCI calculations. However, the spectrum was studied only until 6.5 eV whereas in hypersonics, the spectral region of interest lies between 7.0 - 8.3 eV. In the calculations presented below, vertical energies upto 11 eV are obtained. At the equilibrium geometry of the excited state, the excited state of interest is characterized by an oscillator strength of 1.6517, thereby denoting a very strong transition. The vertical excitation from the ground state at this geometry is 6.4004 eV. At the equilibrium geometry of ground state, the vertical excitation is 6.8367 eV with an oscillator strength 1.8511.

Table 5: $C_4$ optimum bond lengths [A], energy at optimum geometry [eV] measured from the minimum of the ground state, rotational constants [GHz] and normal mode frequencies [$cm^{-1}$] for the excited state of interest, $^3\Sigma_u^-$. The calculation is done using EOM-CCSD[23–25] method.

| Bond Lengths | State $^3\Sigma_u^-$ | Vibration Type | Symmetry | Harmonic Frequency |
|---|---|---|---|---|
| C1=C2 | 1.367 | Symm. stretch | $\sigma_g$ | 2108.0558 |
| C2=C3 | 1.313 | Asymm. stretch | $\sigma_u$ | 1515.6206 |
| C3=C4 | 1.367 | Symm. stretch | $\sigma_g$ | 830.7741 |

| | | | | |
|---|---|---|---|---|
| ∠C1-C2-C3 | 180 | Bending, Zig-Zag | $\pi_g$ | 660.5701 |
| ∠C2-C3-C4 | 180 | Bending, Zig-Zag | $\pi_g$ | 660.5649 |
| | | Scissoring, Outer C-C | $\pi_u$ | 170.2510 |
| | | Scissoring, Outer C-C | $\pi_u$ | 170.2412 |
| Electronic Energy | 6.5911 | | | |
| Rotational Constant | 4.749842 | | | |

The potential energy curves for $C_4$ are obtained for three degrees of freedom which include the variation of bond length of the outer C-C bonds symmetrically, asymmetric stretch of the outer C-C bonds and finally symmetric bending of the outer C-C bonds. The potential energy curves obtained are shown in Fig. 3. An important feature to note is that there are several allowed crossing of the potential energy curves in the low lying electronic states. In asymmetric stretching mode, there are avoided crossings marked in the figure. In the case of symmetric bending of the molecule, as the molecule is bent, we observe symmetric breakdown leading to separation of degenerate states.

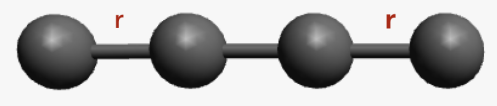


(a) $C_4$ Molecule Schematic

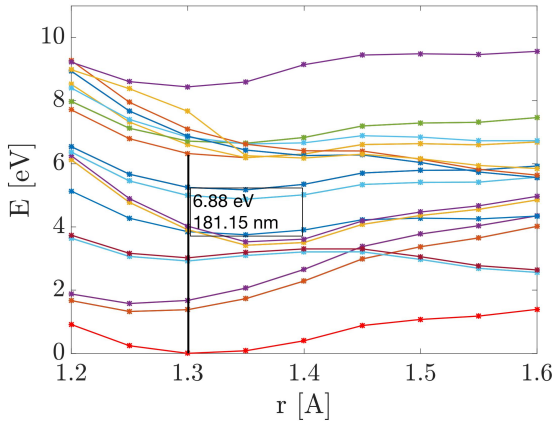


(b) Stretching potential for both outer C-C bond lengths for linear molecule

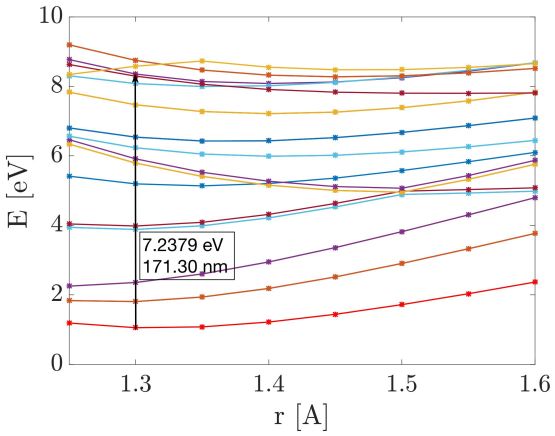


(c) Stretching potential one outer C-C bond length for linear molecule

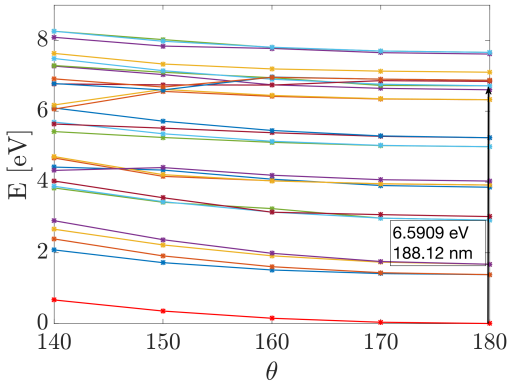


(d) Bending potential for outer C-C-C bond angles

Figure 3: Excited Electronic States potential for $C_4$ computed using EOM-CCSD

Table 6: Comparison of energies [eV] obtained from the EOM-CCSD and MRCI[12] method measured from the ground state minimum.

| State | MRCI[12] | EOM-CCSD | $f_{MRCI}$[12] | $f_{EOM}$ |
|---|---|---|---|---|
| $^3\Sigma_g^-$ | 0.0 | 0.0 | - | - |
| $^3\Pi_g$ | 0.74 | 1.41 | - | - |
| $^3\Pi_u$ | 0.97 | 1.71 | 0.002 | 0.0037 |

| | | | | |
|---|---|---|---|---|
| $^3\Sigma_u^+$ | 1.42 | **M** | - | - |
| $^3\Delta_u$ | 2.78 | 2.94 | - | - |
| $^3\Sigma_u^+$ | 2.85 | 3.04 | - | - |
| $^3\Sigma_u^-$ | 3.35 | 3.84 | 0.0005 | 0.0066 |
| $^3\Delta_u$ | 3.65 | 3.85 | - | - |
| $^3\Sigma_u^+$ | 3.70 | 3.96 | - | - |
| $^3\Pi_u$ | 3.82 | 4.98 | 0.0001 | 0.0032 |
| $^3\Pi_g$ | 4.03 | 5.23 | - | - |
| $^3\Sigma_u^+$ | 4.20 | **M** | - | - |
| $^3\Pi_u$ | 4.53 | 6.33 | 0.007 | 0.0518 |
| $^3\Pi_g$ | 4.78 | 6.70 | - | - |
| $^3\Phi_u$ | 5.01 | **M** | - | - |
| $^3\Sigma_u^-$ | 5.21 | 6.81 | 1.2 | 1.71 |
| $^3\Pi_u$ | 5.28 | 6.82 | 0.045 | - |

In table 6 energies are compared to MRCI energy values at the ground state optimum geometries compute in Ref. 12. When looking at the state of interest with the oscillator strength of 1.2, the MRCI energy is 5.21 eV which the EOM-CCSD energy is 6.71 eV. This difference of about 1.5 eV is also observed in the calculations for $C_3$ in the higher electronic states. This results due to EOM method being a single reference method as opposed to MRCI. The comparison is similar for TD energies as well. However, here it should be recalled that the atomic orbital (AO) basis set used for the EOM-CCSD calculations is aug-cc-pVTZ. On the other hand, the MRCI calculations[12] are done using an AO basis set which consists of 9s5p gaussians in a 5s3p contraction along with an additional d polarization function with an exponent of $\alpha = 0.75$.

### 3.3.3 $C_4H$

Another molecule of interest is the linear isomer of $C_4H$ molecule. Preliminary calculations of $C_4H$ have revealed two strong transitions in the VUV region. The main transition of interest in this molecule is from the doublet ground state, $^2\Sigma^+$, to the excited state having an energy of 7.0061 eV above the ground state, $^2\Sigma^+$. The molecule has a linear ground state optimum geometry. A geometry optimization is also carried out for the two excited electronic states of interest. The first SoI has a bent geometry. The CCH bond angle, as seen in Table 7, is 128° at the optimized geometry. The different vibrational modes are shown in figure 5. As for the second SoI, even after a thorough search of the PES, we have been unable to get an optimum value for the geometry.

The potential energy curves for this molecule are obtained for a varying C-H bond angle '$\theta$' as well as varying bond lengths for the C-H bond. It is observed from Figure 4c that symmetry breakdown occurs as the bond angle is lowered, lowering the symmetry group of the molecule. However, varying the C-H angle alone does not lead to significant variations in the potential energy curves.

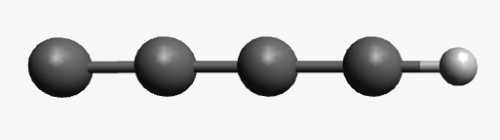

(a) $C_4H$ Molecule Schematic

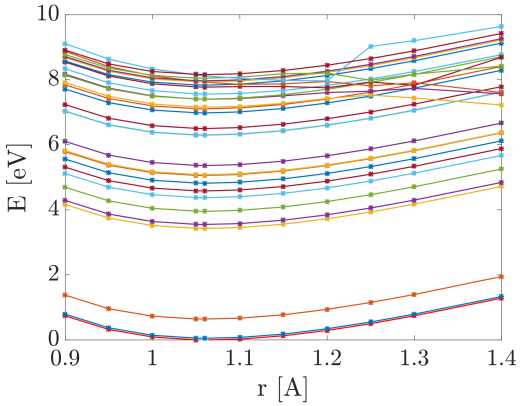


(b) Stretching potential for C-H bond length for linear geometry

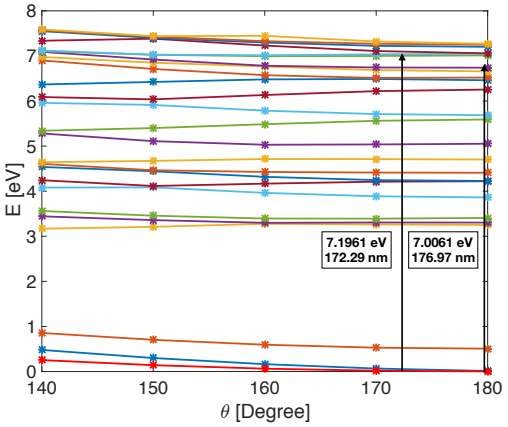


(c) Bending potential for C-H bond angle

Figure 4: Excited Electronic States potential for $C_4H$ computed using EOM-CCSD

Table 7: $C_4H$ optimum bond lengths [A], energy at optimum geometry [eV], rotational constants [GHz] and normal mode frequencies [$cm^{-1}$] for the excited state of interest, $^2\Sigma_u^+$. The ground state (GS) optimum geometry is given as well. The calculation is done using EOM-CCSD[23–25] method.

| Bond Lengths | GS $^2\Sigma_g^+$ | SoI $^2\Sigma_u^+$ | Vibration Type | Symmetry | Harmonic Frequency |
|---|---|---|---|---|---|
| C1≡C2 | 1.2821 | 1.3641 | Asymm. Stretching | a' | 3007.9834 |
| C2-C3 | 1.3279 | 1.3523 | Asymm. Stretching | a' | 1817.4943 |
| C3≡C4 | 1.2229 | 1.3421 | Asymm. Stretching | a' | 1428.3638 |
| C4-H | 1.0625 | 1.0991 | Bending | a' | 845.4424 |
| ∠C1-C2-C3 | 180.0 | 185.73 | Twisting | a" | 612.3218 |
| ∠C2-C3-C4 | 180.0 | 182.42 | Bending, Zig-Zag | a' | 607.4045 |
| ∠C3-C4-H | 180.0 | 128.83 | Bending, Zig-Zag | a' | 311.3956 |
| | | | Scissoring | a' | 206.2718 |
| | | | Twisting | a" | 186.9008 |
| Electronic Energy | 0.0 | 6.22 | | | |
| Rotational Constant | 764.42365 | 4.31932 | 4.29505 | | |

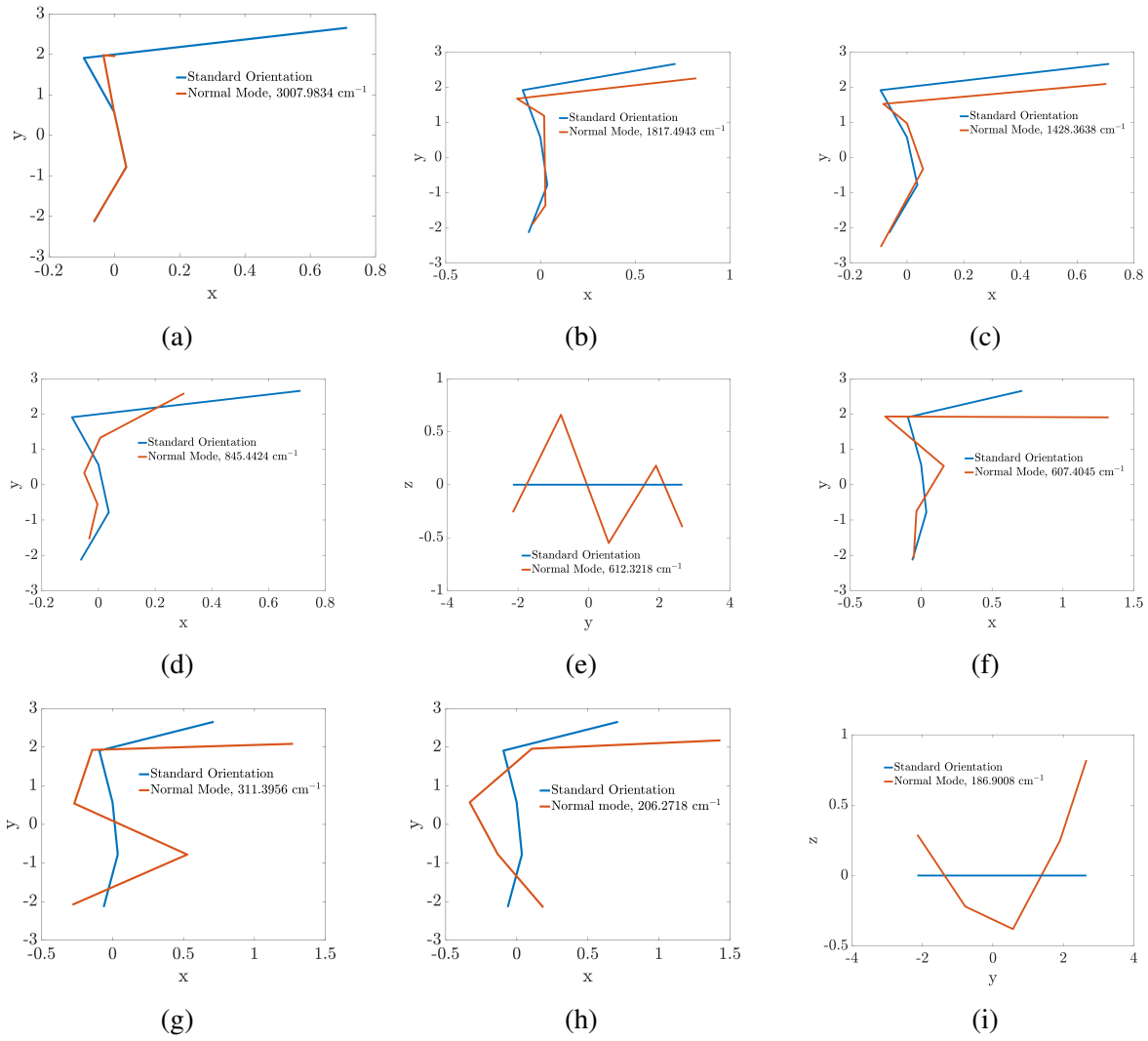


Figure 5: Vibrational normal modes for the state of interest of $C_4H$ shown in Table 7. The blue line represents the optimal geometry plotted in the standard orientation and the orange lines show the bonds are distortion due to vibrations.

## 3.4 Equilibrium composition analysis

Finally, we look at the equilibrium composition for pure carbon mixtures and perform two comparisons of the results obtained. The first is with an experimental result from Gingerich et al.[7] In the paper by Gingerich et al.,[7] the heats of formation of linear carbon clusters were determined using high-temperature Knudsen effusion mass spectrometric method. Table 8 shows a comparison of the heats of formation of the current work and Ref. 7. As can be seen, although the heats of for-

mation from theoretical predictions are close to the experimental results, the experimental results have large uncertainties which lead to significant differences in the mole fractions of the species, Fig. 6. It should be noted here that the equilibrium calculation for both cases are computed using PLATO. We obtain different compositions as a result of using the corresponding heats of formation from our calculations and Ref. 7.

In figure 6, the composition obtained using our calculation is denoted by the solid line and the dashed, dashed dotted and dotted lines represent the equilibrium mole fractions obtained using the heats of formation and their lower and upper bounds respectively, given by Gingerich et al.[7] Looking at the mole fractions, differences primarily lie in the mole fractions of $C_4$ and $C_6$ molecules.

Table 8: Heat of Formation Comparison with Gingerich *et al.*[7]

| $\Delta_f H^o$ [kcal mol$^{-1}$] | $C_2$ | $C_3$ | $C_4$ | $C_5$ | $C_6$ |
|---|---|---|---|---|---|
| Gingerich (1994) | 195.27 $\pm$ 1.91 | 198.61 $\pm$ 3.11 | 251.43 $\pm$ 3.82 | 258.37 $\pm$ 3.82 | 313.58 $\pm$ 4.30 |
| This work | 196.47 | 194.73 | 252.40 | 253.48 | 290.09 |

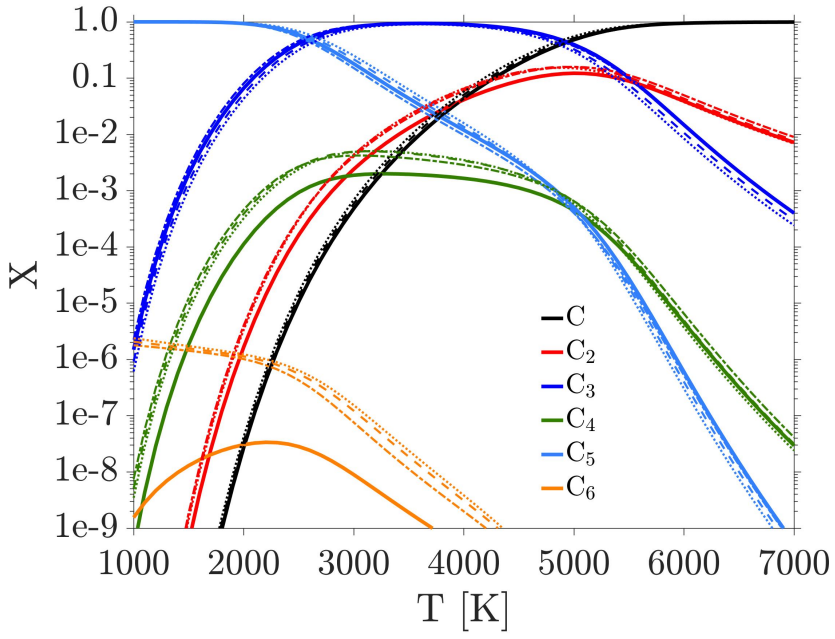


Figure 6: Equilibrium mole fractions for linear carbon clusters at 1 atm pressure, a comparison with Gingerich *et al.*[7]

Another important feature to be noted is the contribution of the rhombic $C_4$ isomer which is very close in energy to the ground state triplet linear isomer of $C_4$. In the experiments by Gingerich et al.,[7] the rhombic structure was neglected based on the results by Slanina.[45] However, as shown in Fig. 7, the addition of the $^1A_g$ state contributes a 28% increase in the mole fractions of $C_4$ for the same equilibrium calculation described earlier in this subsection. In this figure, the other species are not shown for the purpose of clarity.

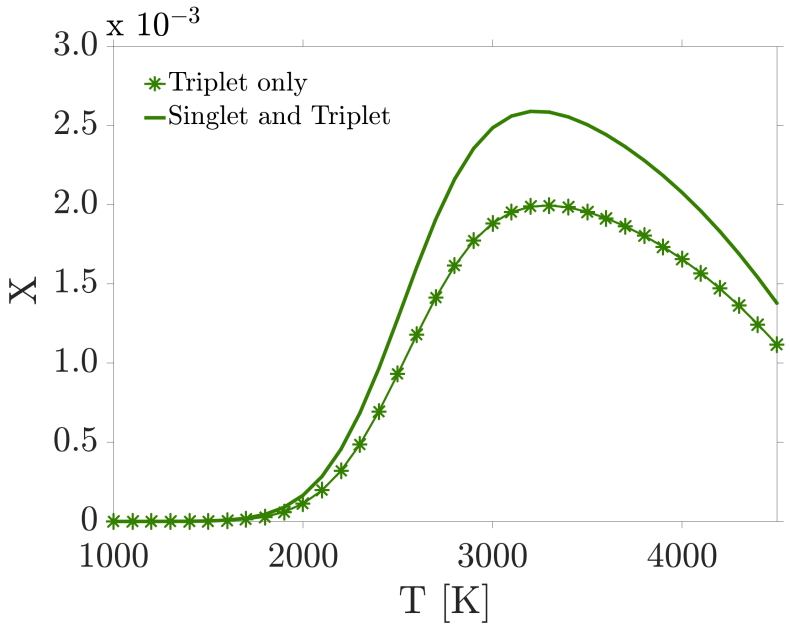


Figure 7: Focusing on the contribution of triplet and singlet $C_4$ isomers

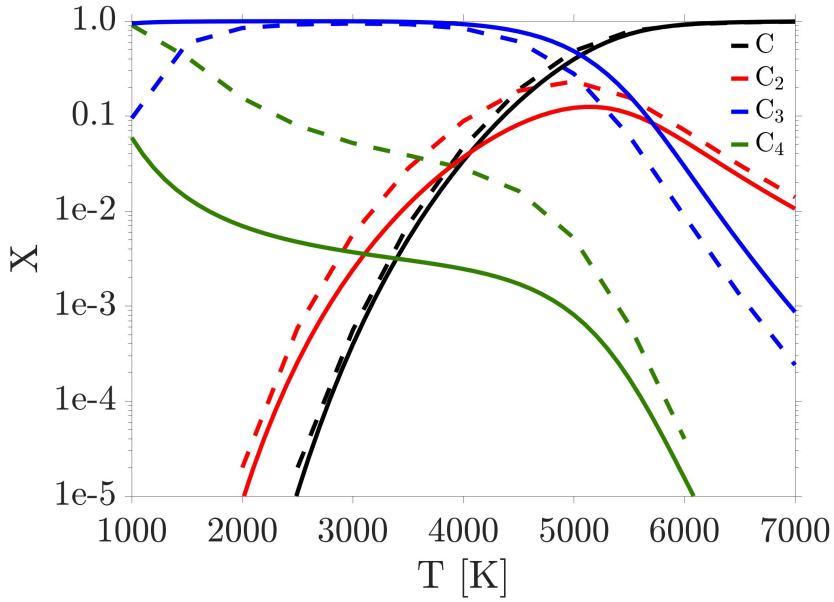


Figure 8: Comparison of equilibrium mole fractions of pure carbon vapor between CEA[46](dashed line) and this work(solid line) at 15000 Pa

The second comparison of equilibrium composition for a pure carbon vapor at 15000 Pa is done with results obtained from CEA[46] thermodynamic database, Fig. 8. The solid lines represent the calculation with the thermodynamic database generated in this paper and the dashed line is the result obtained using data from the CEA thermodynamic database. With the CEA database run, it is observed that the $C_4$ equilibrium mole fraction at lower temperature is higher than that of $C_3$. Here, it should be recalled that at low temperatures, it is a well known fact that $C_3$ is a more stable carbon cluster when compared to $C_2$ and $C_4$ which reaffirms the fact that the CEA database[46] for larger carbon cluster is extremely inaccurate especially at high temperatures. Apart from this behavior, overall, there is significant difference in the mole fractions of the $C_4$ molecule which affects the composition of the whole mixture leading to differences in mole fractions for other molecules like $C_2$. These differences are again attributed to the differences in the thermodynamics data of the molecules being studied.

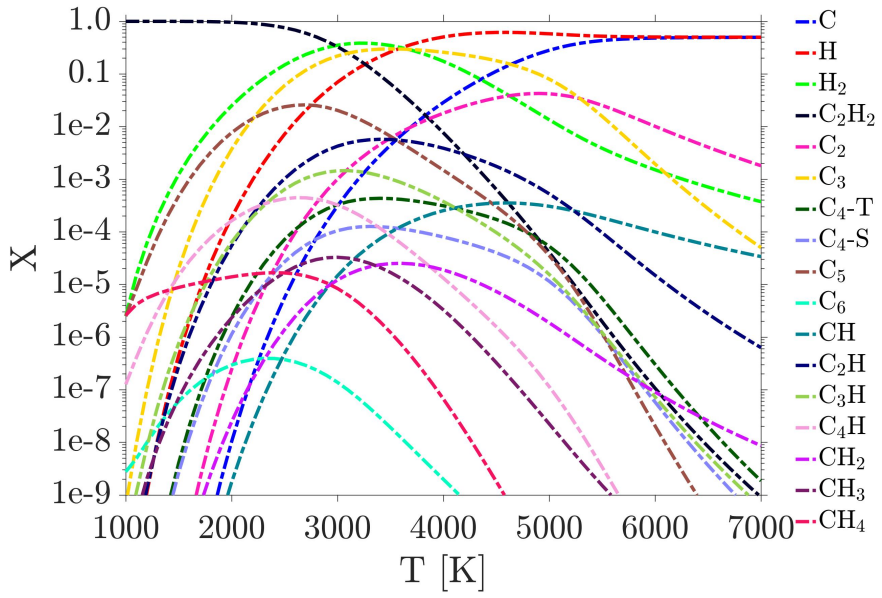


Figure 9: Equilibrium mole fractions of pure acetylene vapor at 1 atm

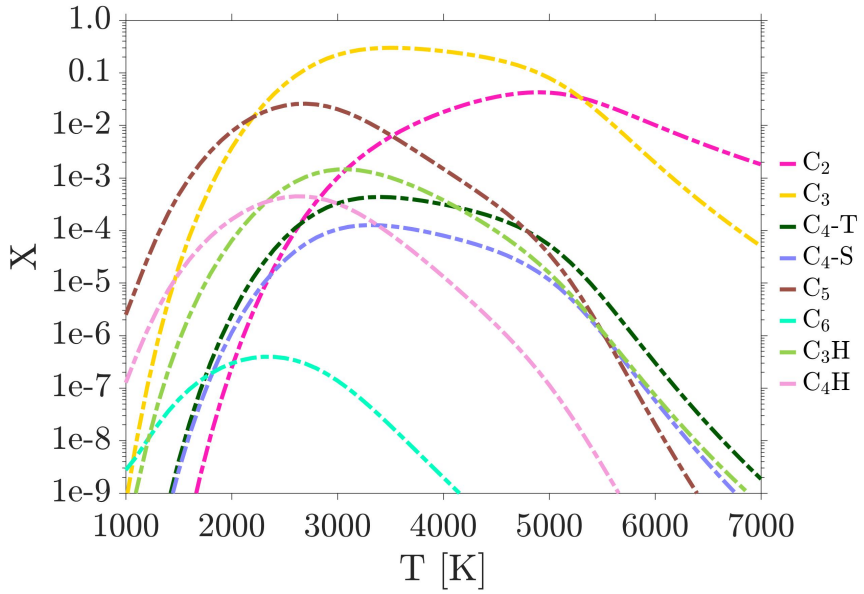


Figure 10: Equilibrium mole fractions of pure acetylene vapor at 1 atm (filtered view)

For the final comparison, the list of species included and thus studied in this work are cataloged in Table 9. These species are necessary to obtain correct equilibrium mixture composition composition. For the even numbered clusters, both the ground state and the low lying singlet state properties are computed. For some hydrocarbons like $C_4H$ with energitically close isomers, properties of all isomers are determined.

Table 9: Species List

| | | | | | | | |
|---|---|---|---|---|---|---|---|
| C | H | $H_2$ | $C_2$ | $C_3$ | $C_4$ | $C_5$ | $C_6$ |
| CH | $C_2H$ | $C_3H$ | $C_4H$ | $CH_2$ | $CH_3$ | $CH_4$ | $C_2H_2$ |

This equilibrium calculation is done for a pure acetylene vapor at a pressure of 1 atm. The species considered for this calculation are the ones listed in Table 9. It should be recalled that the thermodynamic properties of all these molecules have been calculated in this work using the W1 method. The inspiration of using an acetylene vapor is from the shock tube experiments done by Shinn and Park[17] in the 1980s to study the optical properties of $C_3$ and $C_2H$. Although the experiments used a mixture of 99% Argon and 1% $C_2H_2$ at an initial pressure of 0.76 kPa, we do not use the same conditions since the aim of this calculation is to see the relative mole fractions of various carbon clusters and hydrocarbons. Looking at the filtered view of the equilibrium calculations, it is evident that $C_2$, $C_3$, $C_4$ and $C_4H$ are important species especially when considering their impact on absorption of radiation in the boundary layer. The mole fractions of these four species is non-negligible and in future, we wish to quantify the amount of radiation absorption that these molecules would lead to using coupled CFD-Radiation calculations.

# 4 Conclusions

In summary, this work provides a quantitative study of the ground and excited electronic states of the carbon clusters focusing particularly on ablation applications. We use the Guassian16 Software Package[22] to compute the ground state thermochemistry and excited electronic states. We perform a geometry optimization of the excited electronic states of molecules of interest during ablation. Following this, the effects of excited electronic states on the partition function and hence the thermodynamic properties are studied. Finally, the equilibrium compositions for various mixtures are studied using the state-of-the-art databases and the databases developed in this paper. A major take away of this paper is the large difference in heats of formation obtained from the state of the art thermodynamic tables and the new ab-initio data computed in this paper. Another im-

portant highlight is the errors encountered in the thermodynamics upon neglecting the effects of low lying electronic states at these high temperatures. The differences amount up to 11%. Further, it is found that $C_4$ and $C_4H$ have electronic transitions with large oscillator strengths in the VUV region. The optimized geometry of excited electronic state of interest of $C_4$ ($^3\Sigma_u^-$) has a linear structure whereas the excited electronic state of $C_4H$ has a bent geometry. Finally, comparison of the equilibrium mole fractions using the new ab-initio data versus state-of-the-art high temperature thermodynamic tables show significant deviations from each other. These differences are up to an order of magnitude for the $C_4$ molecule and are solely attributed to the large differences in the heats of formation. The paper also emphasizes the need to include the liner triplet and rhombic singlet isomers of $C_4$ in calculations since addition of the rhombic isomer increased the total equilibrium mole fraction of the $C_4$ molecule by 28%.

## Acknowledgement

The work was supported by NASA's ESI grant no. 80NSSC19K0218 with Prof. Marco Panesi as the Principal Investigator. The views and conclusions contained herein are those of the authors and should not be interpreted as necessarily representing the official policies or endorsements, either expressed or implied, of NASA or the U.S. government. The authors would like to thank Dr. Bruno Lopez and Dr. Alessandro Munafo for providing the ROSSDAG and PLATO codes to compute thermodynamics properties and equilibrium compositions presented in this work.

## References

(1) Pitzer, K. S.; Clementi, E. Large molecules in carbon vapor. *Journal of the American Chemical Society* **1959**, *81*, 4477–4485.

(2) Clementi, E. Electronic States in the $C_4$ Molecule. *Journal of the American Chemical Society* **1961**, *83*, 4501–4505.

(3) Raghavachari, K.; Binkley, J. Structure, stability, and fragmentation of small carbon clusters. *The Journal of Chemical Physics* **1987**, *87*, 2191–2197.

(4) Martin, J. M. L.; François, J.-P.; Gijbels, R. Ab-initio study of the structure, infrared spectra, and heat of formation of C4. *The Journal of Chemical Physics* **1991**, *94*, 3753–3761.

(5) Martin, J.; François, J.-P.; Gijbels, R. On the heat of formation of $C_5$ and higher carbon clusters. *The Journal of Chemical Physics* **1991**, *95*, 9420–9421.

(6) Martin, J. M.; Taylor, P. R. Structure and vibrations of small carbon clusters from coupled-cluster calculations. *The Journal of Physical Chemistry* **1996**, *100*, 6047–6056.

(7) Gingerich, K. A.; Finkbeiner, H. C.; Schmude Jr, R. W. Enthalpies of formation of small linear carbon clusters. *Journal of the American Chemical Society* **1994**, *116*, 3884–3888.

(8) Van Orden, A.; Saykally, R. J. Small carbon clusters: spectroscopy, structure, and energetics. *Chemical Reviews* **1998**, *98*, 2313–2358.

(9) Karton, A.; Tarnopolsky, A.; M. L. Martin, J. Atomization energies of the carbon clusters Cn (n=2-10) revisited by means of W4 theory as well as density functional, Gn, and CBS methods. *Molecular Physics* **2009**, *107*, 977–990.

(10) Schmidt, T. W. The Spectroscopy of $C_2$: A Cosmic Beacon. *Accounts of Chemical Research Special Issue "Astrochemistry and Planetary Science"* **2021**,

(11) Pacchioni, G.; Koutecký, J. Ab-initio MRD CI investigation of the optical spectra of $C_4$ and $C_5$ clusters. *The Journal of Chemical Physics* **1988**, *88*, 1066–1073.

(12) Mühlhäuser, M.; Froudakis, G. E.; Hanrath, M.; Peyerimhoff, S. D. The electronic spectrum of linear and rhombic $C_4$. *Chemical Physics Letters* **2000**, *324*, 195–200.

(13) Graf, S.; Geiss, J.; Leutwyler, S. Ab initio calculations of excited states in $C_4H$ and implications for ultraviolet photodissociation. *The Journal of Chemical Physics* **2001**, *114*, 4542–4551.

(14) Fortenberry, R. C.; King, R. A.; Stanton, J. F.; Crawford, T. D. A benchmark study of the vertical electronic spectra of the linear chain radicals $C_2H$ and $C_4H$. *The Journal of Chemical Physics* **2010**, *132*, 144303.

(15) Brandis, A. M.; Johnston, C. O.; Cruden, B. A.; Prabhu, D. K. Equilibrium Radiative Heating from 9.5 to 15.5 km/s for Earth Atmospheric Entry. *Journal of Thermophysics and Heat Transfer* **2016**, *31*, 178–192.

(16) Prakash, S.; Park, C. Shock Tube Spectroscopy of $C_3$+$C_2H$ Mixture in the 140-700 nm Range. *AIAA Paper* **1979**, *79-0094*.

(17) Shinn, J. L. Optical Absorption of Carbon and Hydrocarbon Species from Shock-Heated Acetylene and Methane in the 135-220 nm Wavelength Range. *Prog. Astron. Aeronaut.* **1982**, *82*, 68–80.

(18) Jaffe, R. L.; Chaban, G.; Schwenke, D. Theoretical Determination of High-Temperature Absorption Spectra for $C_3$ in the Near-UV and VUV. $43^{rd}$ AIAA Thermophysics Conference. 2012; p 2743.

(19) Park, C.; Jaffe, R. L.; Partridge, H. Chemical-kinetic parameters of hyperbolic earth entry. *Journal of Thermophysics and Heat transfer* **2001**, *15*, 76–90.

(20) Monninger, G.; Förderer, M.; Gürtler, P.; Kalhofer, S.; Petersen, S.; Nemes, L.; Szalay, P. G.; Krätschmer, W. Vacuum ultraviolet spectroscopy of the carbon molecule $C_3$ in matrix isolated state: experiment and theory. *The Journal of Physical Chemistry A* **2002**, *106*, 5779–5788.

(21) Martin, J. M. L.; de Oliveira, G. Towards standard methods for benchmark quality ab initio thermochemistry-W1 and W2 theory. *The Journal of Chemical Physics* **1999**, *111*, 1843–1856.

(22) Frisch, M. J.; Trucks, G. W.; Schlegel, H. B.; Scuseria, G. E.; Robb, M. A.; Cheeseman, J. R.;

Scalmani, G.; Barone, V.; Petersson, G. A.; Nakatsuji, H.; others, . Gaussian 16, Revision A. 03, Gaussian, Inc., Wallingford, Ct. 2016.

(23) Koch, H.; Jørgensen, P. Coupled cluster response functions. *The Journal of Chemical Physics* **1990**, *93*, 3333–3344.

(24) Stanton, J. F.; Bartlett, R. J. The equation of motion coupled-cluster method. A systematic biorthogonal approach to molecular excitation energies, transition probabilities, and excited state properties. *The Journal of Chemical Physics* **1993**, *98*, 7029–7039.

(25) Kállay, M.; Gauss, J. Calculation of excited-state properties using general coupled-cluster and configuration-interaction models. *The Journal of Chemical Physics* **2004**, *121*, 9257–9269.

(26) Sharma, M. P.; Jaffe, R. L.; Munafò, A.; Panesi, M. Calculation of Thermochemical Properties of Carbon-cluster Ablation Species. 2018 Joint Thermophysics and Heat Transfer Conference. 2018; p 4179.

(27) Curtiss, L. A.; Raghavachari, K.; Trucks, G. W.; Pople, J. A. Gaussian-2 theory for molecular energies of first-and second-row compounds. *The Journal of Chemical Physics* **1991**, *94*, 7221–7230.

(28) Curtiss, L. A.; Raghavachari, K.; Redfern, P. C.; Rassolov, V.; Pople, J. A. Gaussian-3 (G3) theory for molecules containing first and second-row atoms. *The Journal of Chemical Physics* **1998**, *109*, 7764–7776.

(29) Curtiss, L. A.; Redfern, P. C.; Raghavachari, K. Gaussian-4 theory. *The Journal of Chemical Physics* **2007**, *126*, 084108.

(30) Gurvich, L. V.; Veits, I. V.; Alcock, C. B. *Thermodynamics properties of individual substances. Volume 1-Elements O, H/D, T/, F, Cl, Br, I, He, Ne, Ar, Kr, Xe, Rn, S, N, P, and their compounds. Part 1-Methods and computation. Part 2-Tables*; Hemisphere Publishing Corp., New York, 1989.

(31) Alberti, A.; Munafò, A.; Koll, M.; Nishihara, M.; Pantano, C.; Freund, J. B.; Elliott, G. S.; Panesi, M. Laser-induced non-equilibrium plasma kernel dynamics. *Journal of Physics D: Applied Physics* **2019**, *53*, 025201.

(32) Munafò, A.; Alberti, A.; Pantano, C.; Freund, J. B.; Panesi, M. A computational model for nanosecond pulse laser-plasma interactions. *Journal of Computational Physics* **2020**, *406*, 109190.

(33) Becke, A. D. Becke's three parameter hybrid method using the LYP correlation functional. *The Journal of Chemical Physics* **1993**, *98*, 5648–5652.

(34) Dunning Jr, T. H. Gaussian basis sets for use in correlated molecular calculations. I. The atoms boron through neon and hydrogen. *The Journal of Chemical Physics* **1989**, *90*, 1007–1023.

(35) Kendall, R. A.; Dunning Jr, T. H.; Harrison, R. J. Electron affinities of the first-row atoms revisited. Systematic basis sets and wave functions. *The Journal of Chemical Physics* **1992**, *96*, 6796–6806.

(36) Curtiss, L. A.; Raghavachari, K.; Redfern, P. C.; Pople, J. A. Assessment of Gaussian-2 and density functional theories for the computation of enthalpies of formation. *The Journal of Chemical Physics* **1997**, *106*, 1063–1079.

(37) Ruscic, B.; Pinzon, R. E.; Morton, M. L.; von Laszevski, G.; Bittner, S. J.; Nijsure, S. G.; Amin, K. A.; Minkoff, M.; Wagner, A. F. Introduction to active thermochemical tables: Several "key" enthalpies of formation revisited. *The Journal of Physical Chemistry A* **2004**, *108*, 9979–9997.

(38) Ruscic, B.; Pinzon, R. E.; von Laszewski, G.; Kodeboyina, D.; Burcat, A.; Leahy, D.; Montoy, D.; Wagner, A. F. Active thermochemical tables: thermochemistry for the 21st century. Journal of Physics: Conference Series. 2005; p 561.

(39) Ruscic, B. Active Thermochemical Tables (ATcT) values based on ver. 1.118 of the Thermochemical Network, 2015. *available at ATcT. anl. gov* **2016**,

(40) Stull, D. R.; Prophet, H. *JANAF thermochemical tables*; 1971.

(41) Gurvich, L. V.; Veyts, I. *Thermodynamic Properties of Individual Substances: Elements and Compounds*; CRC press, 1990; Vol. 2.

(42) Huber, K.-P. *Molecular spectra and molecular structure: IV. Constants of diatomic molecules*; Springer Science & Business Media, 2013.

(43) Werner, H.; Knowles, P. J.; Knizia, G.; Manby, F. R.; Schütz, M. Molpro: A general-purpose quantum chemistry program package. *Wiley Interdisciplinary Reviews: Computational Molecular Science* **2012**, *2*, 242–253.

(44) Watts, J. D.; Gauss, J.; Stanton, J. F.; Bartlett, R. J. Linear and cyclic isomers of $C_4$. A theoretical study with coupled-cluster methods and large basis sets. *The Journal of Chemical Physics* **1992**, *97*, 8372–8381.

(45) Slanina, Z. An estimation of the energy difference between the linear and rhombic structures of $C_4$(g). *Chemical Physics Letters* **1990**, *173*, 164–168.

(46) McBride, B. J.; Gordon, S.; Reno, M. A. Coefficients for calculating thermodynamic and transport properties of individual species. **1993**,